

Numerical Modeling of the Effects of Kizildere Geothermal Power Plant on Water Quality of the Great Menderes River, Turkey

Şebnem Elçi¹, Adem Erdem¹ and Gulden Gokcen²

¹Department of Civil Engineering, Izmir Institute of Technology, Urla, Izmir, Turkey

²Department of Mechanical Engineering, Izmir Institute of Technology, Urla, Izmir, Turkey

sebnemelci@iyte.edu.tr, ademerdem@iyte.edu.tr, guldengokcen@iyte.edu.tr

Keywords: Numerical modeling, WASP model, Kizildere Geothermal Power Plant, Turkey, water quality

ABSTRACT

Although geothermal energy is considered as one of the cleaner forms of energy, discharge of the power plant's effluent into nearby streams impacts the environment which requires special attention. Motivated by high boron concentrations observed in crops and soils of a river basin located in the south-west of Turkey, this study is investigated the effects of Kizildere Geothermal Power Plant on water quality of the Great Menderes River.

In this study, first the hydrodynamic model was validated with the discharge measurements conducted by Electrical Power Resources Survey and Development Administration (EIEI) and State Hydraulic Works (DSI) in five different stations within the modeled segment of the river. After validation of the hydrodynamics along the river, dissolved oxygen (DO), nutrients (ammonia and nitrate), metals (Li, As, Sb) and boron were modeled by Water Quality Analysis Simulation Program (WASP 7.2). Then the results were compared to the water quality measurements conducted within the study area. The effect of the Power Plant was investigated via modeling considering two scenarios: with and without the Power Plant discharges introduced into the model as loading.

The simulation results indicated that boron concentrations were significantly affected during winter, when most of the water is kept to increase the upstream reservoir storage. During the same period, when the flows are low; arsenic, lithium, antimony, dissolved oxygen and ammonia concentrations were also significantly affected by the effluent of the Power Plant.

1. INTRODUCTION

Environmental effects of geothermal applications have been studied widely. Geothermal development in the land can result in the pollution of water resources both directly and indirectly. With the consideration of the importance of agricultural activities in the villages and towns, the effects should be assessed in terms of quality of irrigation and domestic water. Re-injection is obliged by laws and regulations in most of the countries with geothermal development. However, re-injection may be complicated by the possibility of reduction in the permeability of the aquifer surrounding the re-injection well by silica deposits from a supersaturated solution. Surface water can be contaminated due to chemical waste disposal or leakage during the operation. In addition to this, the effects of storage of drilling fluids, lubricants, chemicals used for preventing settling, and other special chemicals should also be taken into consideration (Brown, 1995, 2000; Rybach, 2005).

Kizildere Geothermal Power Plant is the first geothermal power plant of Turkey installed with a capacity of 20.4 MW_e in 1984. It is a single flash design with a direct contact condenser. Kizildere Geothermal Field is a liquid dominated system with a reservoir temperature of 200-242°C and a steam fraction of 10-20%. Twenty two production wells have been drilled but only nine of which are being operated.



Figure 1: Kizildere Geothermal Power Plant, general view.

When the geothermal fluid reaches to the wellhead, it is directed to a wellhead separator where steam and liquid phases are separated. Then steam with an average flow rate of 33.3 kg/s is sent to the turbine where the electrical power is maintained, while 257.7 kg/s liquid, which is 88.5% of the total flow rate, is used for district heating system of a town nearby, rejected to the Great Menderes River through a 1.8-km long channel and a small fraction of the liquid is injected back to the reservoir since 2002 by the Well R2 (Gokcen and Yildirim, 2008; Yildirim Ozcan and Gokcen, 2009).

WASP 7.2 (Water Quality Analysis Simulation Program) developed by US Environmental Protection Agency (EPA) is designed for aquatic systems includes both the water column and the underlying benthos in 1, 2, and 3 dimensional systems and solves for the advection, dispersion, point and diffuse mass loading and boundary exchange processes. The model utilizes the kinematic wave model for flows but, when it is needed, it can also be linked with other hydrodynamic and sediment transport models.

In this study, the effects of Kizildere Geothermal Power Plant on water quality of the Great Menderes River are modeled by WASP 7.2. Following the verification of the hydrodynamic model, dissolved oxygen (DO), ammonia (NH₃), nitrate (NO₃), metals (Li, As, Sb), boron concentrations, and solids are modeled by utilizing eutrophication and organic toxicant modules of WASP 7.2 and the results were compared with monthly water quality

measurements. The effects of the effluent of Kizildere Geothermal Power Plant are investigated by modeling of the pollutant loads of input into the river for two different scenarios; with and without the discharges introduced into the model as loading.

2. NUMERICAL MODEL (WASP 7.2)

The water quality analysis simulation program (WASP), supported and developed by the US Environmental Protection Agency (USEPA), is the multi-dimensional and dynamic water quality modeling program. The model can be used to analyse a variety of water quality problems in ponds, streams, lakes, reservoirs, rivers, estuaries, and coastal waters. The time-varying processes of advection, dispersion, point and diffuse mass loading and boundary exchange are represented in the model. WASP also can be linked with hydrodynamic and sediment transport models that can provide flows, depths, velocities, temperature, salinity and sediment fluxes. WASP contains four layers representing different parts of water ecosystems. These layers are defined as 1) The water column in contact with atmosphere, 2) The water column non-contact with atmosphere, 3) The underlying benthos in contact with water, 4) The sediment bed non-contact with water. When the conservation of mass and momentum are solved for both water and solids between the layers, flow and transport in the water column, transport in the porous media of the bed sediment, transport in the water column via settling/resuspension and transport with rainfall/evaporation are considered. Although the model can not execute hydrologic computations, it can be linked to hydrologic models such as HSPF and SWIMM, and can be linked to hydrodynamic models through input files. When WASP is used alone, it solves the hydrodynamics using the kinematic wave equation. It can also transfer data to the central database system developed by the EPA (Ambrose et al., 1993).

Water quality processes are represented in special kinetic subroutines that are either chosen from a library or written by the user. WASP is structured to permit easy substitution of kinetic subroutines into the overall package to form problem-specific models. WASP7 comes with four modules: TOXI for simulation of toxicants and EUTRO for simulation of conventional water quality including ammonia, nitrate, dissolved oxygen, salinity, organic/inorganic phosphorus, MERCURY for simulation of mercury and HEAT for simulation of temperatures in water bodies.

3. STUDY AREA

Study area was selected as a part of the Great Menderes River, Turkey, where the effluent of Kizildere Geothermal Power Plant is discharged (Figure 2). 584 km long river flows into the Aegean Sea from the west of Lake Bafa by collecting the waters of the Great Menderes Basin having a drainage area of 24,976 km². The river's average flow is approximately 110 m³/sn. The average flow is the highest in January and February (average 164 m³/sn). On the other hand, the flow in the summer is very low. (average 12 m³/sn in August). In rainy years, it was observed that the flow rate exceeds 300 m³/sn and due to the melting of snows in March and April the highest flow rates can be observed during these months flooding the plain. Two dams, Adigüzel (Denizli) and Kemer (Aydin) Dams, are located on the river.

Model boundaries are selected to include the river segment between monitoring stations 7-26 and 7-12 on the main river and the monitoring station on the Çürüksu tributary (7-59) where sampling points and the geothermal plant were located (Figure 3).



Figure 2: Location of the Great Menderes River.

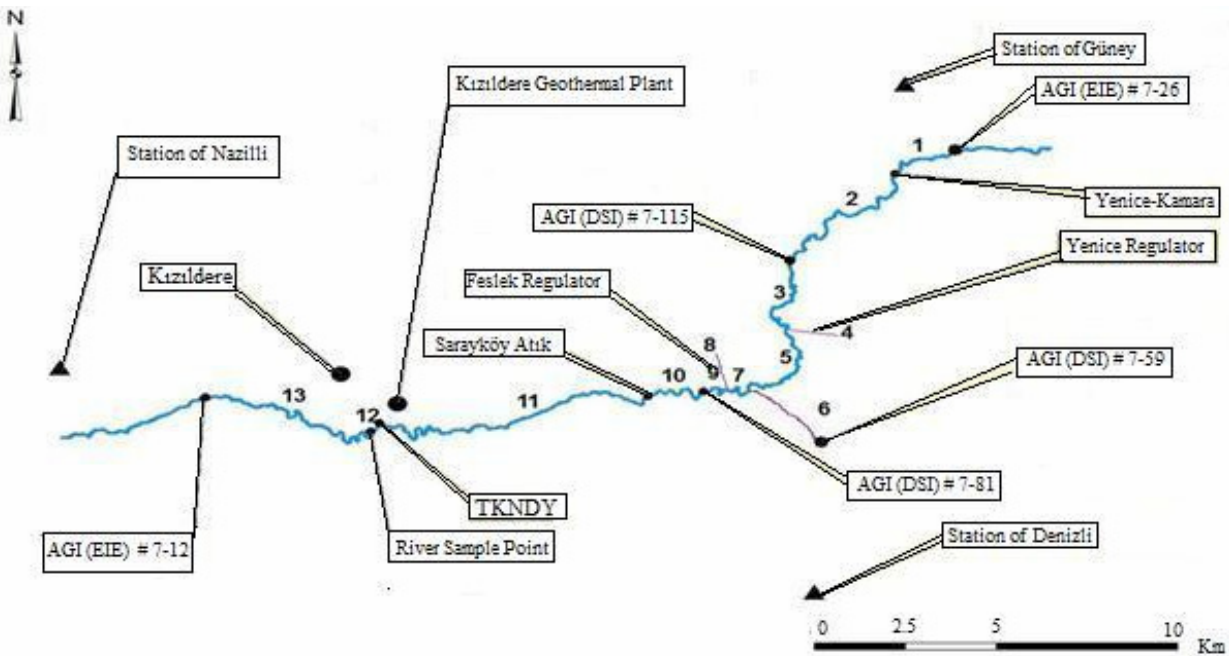


Figure 3: The modeled segments of the Great Menderes River and the locations of monitoring stations.

Table 1: Properties of the river segments used in the model.

Segment Number	Length (m)	Width (m)	Surface Area (m ²)	Depth (m)	Volume (m ³)	Velocity (m/sn)	Slope (°)	Roughness coefficient
1	4771	24	114504	2.50	286260	0.26	0.0052	0.0117
2	12407	28	347396	1.51	524568	0.36	0.0024	0.0117
3	7947	25	198675	1.51	299999	0.41	0.0012	0.0117
4	100	10	1000	1.05	1050	1.47	0.0010	0.0117
5	8046	25	201150	1.51	303737	0.41	0.0012	0.0117
6	16366	18	294588	2.41	709957	0.35	0.0012	0.0117
7	2123	25	53075	0.72	38214	0.86	0.0022	0.0117
8	100	10	1000	1.05	1050	1.47	0.0010	0.0117
9	2222	25	55550	0.72	39996	0.86	0.0023	0.0117
10	4928	27	133056	0.72	95800	0.79	0.0004	0.0117
11	7521	29	218109	1.50	327164	0.35	0.0004	0.0117
12	839	24	20136	1.50	30204	0.43	0.0012	0.0117
13	11914	29	345506	2.28	787754	0.23	0.0003	0.0117

4. IMPLEMENTATION OF THE WATER QUALITY MODEL

Model domain along the river was divided into 13 segments as shown in Figure 3 for the simulation of the hydrodynamics and water quality parameters using the WASP model. Segmentation was based on locations of new sampling points and existing monitoring stations by the State Hydraulic Works (DSI) and Electrical Power

Resources Survey and Development Administration (EIEI) along the river. The new sampling points are shown in Figure 3 and marked as Yenice-Kamara, Saraykoy Atik, TKNDY (where the effluent canal merges into the main river), and river sampling point.

The length and width of the segments were derived from the 1/25000 scale maps and the cross-section details of the

river segments were specified for the monitoring stations. The water depth of the river bed was also derived from the cross-section details and from the measured water levels at the monitoring stations. The surface area and volume for each segment was calculated based on these parameters. The slopes of the segments were calculated by dividing the elevation differences between the segments by the segment length. Table 1 summarizes the properties of the segments used in the numerical model.

Roughness coefficient of the river was calculated by the formula developed Meyer-Peter ve Müller (1948) where roughness coefficient is expressed in terms of grain diameter (Yang, 1996).

$$n = \frac{(d_{90})^{1/6}}{26} \quad (1)$$

The value of d_{90} is found as 0.0008 m from the grain diameter distribution specified for the Great Menderes River and the roughness coefficient is calculated as 0.0117.

In the study area, there are five monitoring stations three of which are operated by DSI (7-115, 7-59, 7-81) and the remaining two are operated by EIEI (7-26 ve 7-12). In these stations daily flow rates and some water quality parameters are monitored. Daily flow rates measured at these stations and the flow rate of the water withdrawn at the two water intakes (Yenice and Feslek) for irrigation are obtained from DSI and EIEI for the simulation period (water year 2006).

There are three meteorological stations close to the study site: Denizli, Nazilli ve Güney meteorological stations, Güney station being the closest. Therefore, daily average air temperature (°C), wind speed (m/s), and solar radiation (cal/cm²) values recorded at this station were used as input data for the numerical model. Since water temperatures were measured at the river monitoring station # 7-12 once a month, to obtain daily values, a relation between measured water values and air temperatures for the same dates were obtained and daily water temperatures were derived from the equation (2).

$$T_w = 0.487 * T_a + 8.6027 \quad (2)$$

where, T_w is the water temperature (°C) and T_a is the air temperature (°C). The values of dissolved oxygen (DO) and total salt concentration were determined by specified methods used in literature. Following Bell et al. (2006) the daily values of the dissolved oxygen (DO) are obtained (Equation (3)).

$$DO = 0.0043 * T_w^2 - 0.36 * T_a + 14.48 \quad (3)$$

where, DO is the dissolved oxygen (ppm), T_w is the water temperature (°C), and T_a is the air temperature (°C). Total concentration of dissolved salts in irrigation water can be obtained from measured electrical conductivity (EC) once the ratio between two parameters is determined from field observations. For monitoring station # 7-12 this ratio was provided as 0.64 by EIEI. Thus, total concentration of dissolved salts can be estimated as (Equation 4):

$$Salinity = 0.64 * EC \quad (4)$$

Measurement of water quality parameters were conducted at several locations (Yenice-Kamara, Menderes tekstil, Sarayköy atik, TKNDY, sampling point N ve Buharkent bridge) within the model domain. Prior to the modeling of water quality parameters, the hydrodynamics part of the model was validated with the observations. For these simulations, eutrophication module was selected and 1-D kinematic wave approach was utilized. Time step was set to 1.44 minute and the discharges were output daily for the whole water year 2006 (10.01.2005-9.30.2006). For the model domain, the segments were specified as input based on the properties summarized in Table 1. The parameters measured at the stations at the beginning of the simulation period were specified in the model as initial conditions. The daily values of air temperature, wind speed, solar radiation, and water temperature were provided as input data for the simulation period.

In flows section, the flow functions showing flow time series at the boundaries of the model were specified using daily flow measurements recorded at the river monitoring stations. In this section, four different flow functions were defined as Yenice-Kamara, Çürüksu, Yenice and Feslek regulators. Water quality measurements were used as boundary conditions in the model. Figure 4 shows the comparison of simulated and measured flow rates at three river monitoring stations (7-115, 7-59, and 7-12). As seen in the figures, simulated results are in agreement with the observed values pointing out the suitability of the numerical model for the river.

5. RESULTS OF THE WATER QUALITY MODEL

Following the simulation of discharges at monitoring stations accurately, water quality parameters were modeled. In the loads section, water quality parameters were specified as input data for model segments according to sampling locations. For instance, parameters observed at Yenice-Kamara were used as input data for segments 1 and 2. Similarly, parameters observed at Menderes tekstil were used for segments 7 and 9, Sarayköy atik for segments 10 and 11, and river sampling points were specified as input data for segments 12 and 13.

Organic toxicant module was used for determination of boron and other contaminants' concentration values in the river. Input data of the module has similarities with the eutrophication module. In the loads and boundary sections, measured concentration values were used as input data. Validation of the water quality model was conducted by comparison of the simulated and observed water temperatures (Figure 5).

Water quality parameters such as dissolved oxygen, salinity and ammonium were simulated by eutrophication module and the results were discussed for different scenarios with and without the discharge of effluent of the geothermal plant to the river. This analysis was conducted by specifying different initial temperature and concentration values in the loads section of the model. Figure 6 presents the effects of the plant on dissolved oxygen, salinity and ammonium. Since dissolved oxygen concentration is directly related to the temperature (Equation 3), when warmer effluent of the plant is discharged into the river, a decrease in dissolved oxygen concentrations is expected. Results also indicated an increase in salinity and ammonia concentrations due to the discharges of the plant (Figure 6).

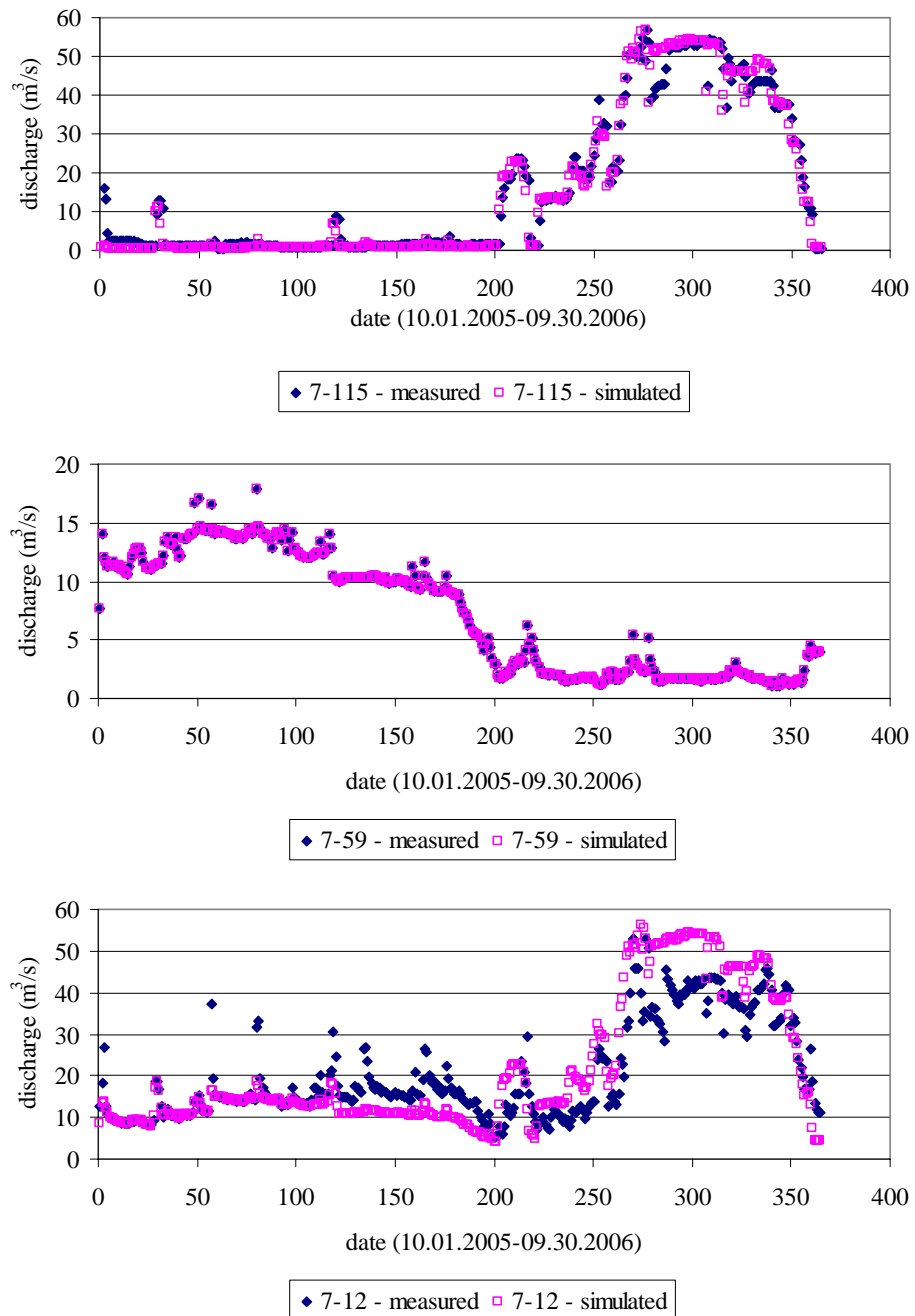


Figure 4: Comparison of the simulated flow rates with the measurements for three river monitoring stations (7-115, 7-59 and 7-12).

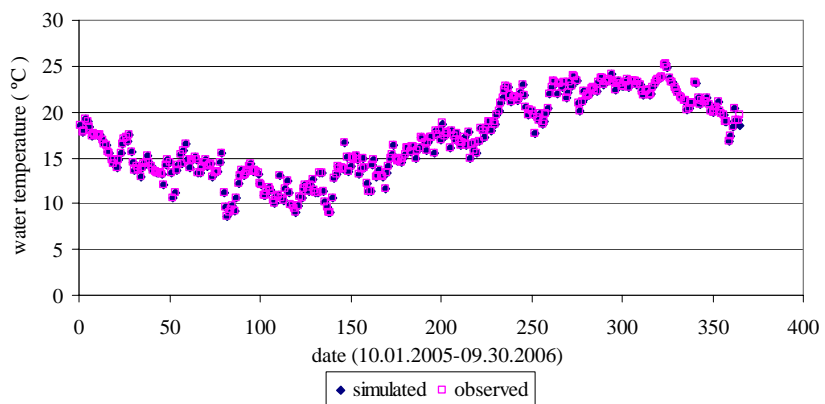


Figure 5: Comparison of the simulated and observed water temperatures at the monitoring station # 7-12.

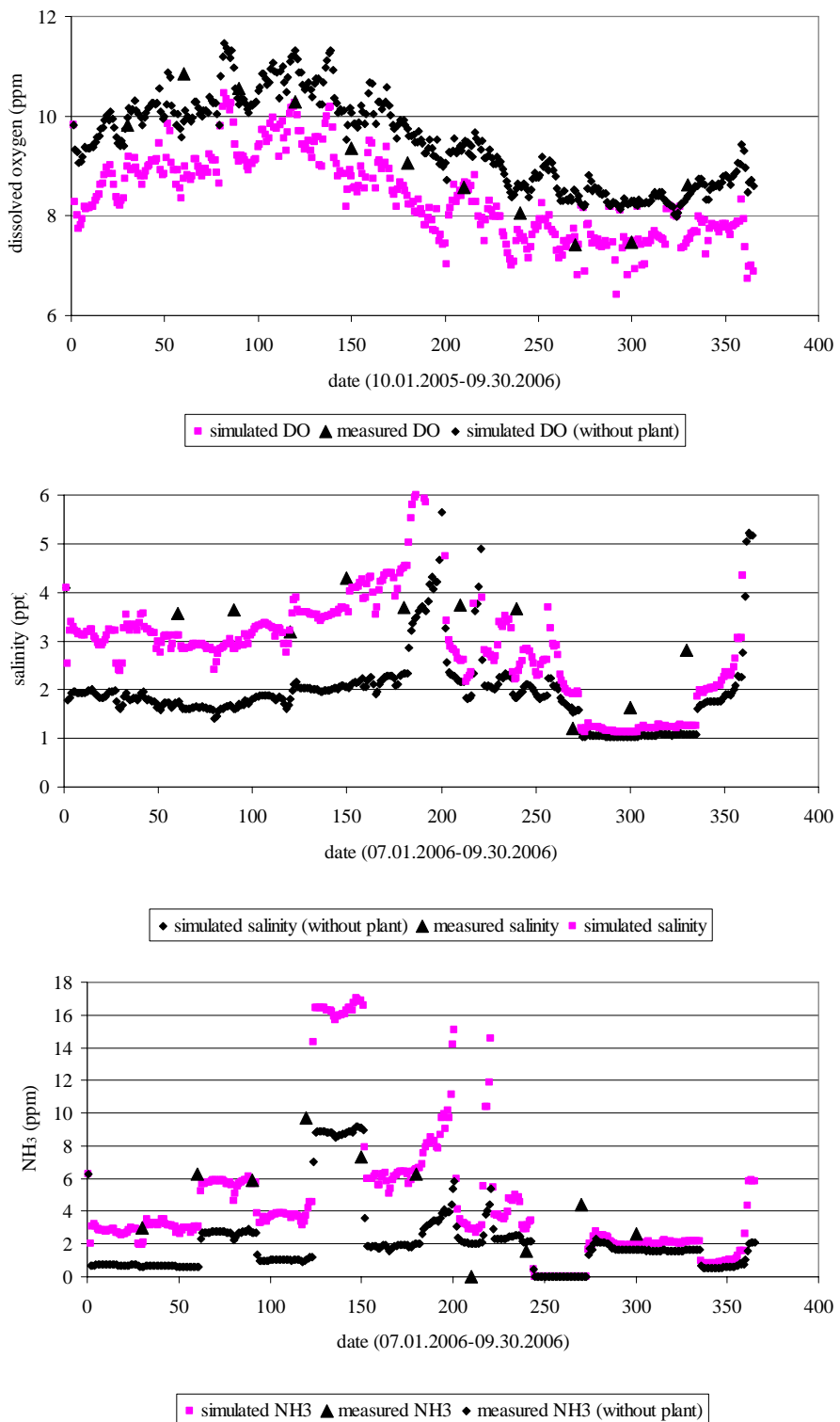


Figure 6: Comparison of the simulated and observed dissolved oxygen, salinity and ammonia concentrations at the 12 segment of the river with and without the plant.

Water and soil samples received water from TKNDY, the merging point of the canal discharging effluent of the plant to the river, indicated deterioration of water quality at this location. Two scenarios; with and without the discharges from the power plant were modeled by introducing measured concentrations as loads at the merging point for the current condition and by excluding loads at the merging point for simulating the condition without the plant.

Effluent of geothermal power plants may have lithium, boric acid, arsenic, mercury and ammonia at low

concentrations. They are also expected to have high salinity and some trace elements at very low concentrations such as silver, selenium, and antimony. However, in the samples retrieved from the study site, no silver or selenium was found.

Boron concentrations were modeled along the river by utilizing the organic toxicant module. Modeling was conducted using two different input data sets. For the first case, simulating the current conditions, the observations at the canal were introduced as loads and for the second case

the input data excluded the concentrations observed at the merging canal. The graphics (Figure 7) illustrate the comparison of the results of these two cases which will be called as with and without plant. As can be seen in the figure, during winter, low flow rates are measured at the monitoring stations (due to the fact that most of the water is diverted to the reservoir) and geothermal plant causes an increase in boron concentrations. During summer, when water is withdrawn from the reservoir and released to the river for irrigation purposes, boron concentrations reduce due to dilution of effluent in the canal with the river. Boron can be absorbed by the suspended particles in water easily, therefore upon settling, accumulation of boron at the river beds, and even accumulation of boron at the irrigated lands can be observed. Indeed, soil samples retrieved from the lands surrounding river indicated high boron concentrations: at the merging canal boron concentrations were as high as 135 ppm, where this amount was 9 ppm at the upstream of the river (Yenice-Kamara) and 38 ppm at Sarayköy atik (Gokcen, 2008).

Arsenic can be found in the effluent of geothermal power plants due to its fast solubility in water. As can be seen in Figure 8, arsenic concentrations increase in low flow conditions (winter) due to the waste waters of the plant. Similar trend was observed in lithium concentrations as well (Figure 9). In the Great Menderes River most of the water is diverted for irrigation of the agricultural lands, and high concentrations of boron and lithium may damage the harvest in these areas.

This study investigated the environmental effects of Kızıldere Geothermal Plant on Büyük Menderes River. The aim was to create awareness on the environmental effects of geothermal plants, although it still remains as one of the clean sources of energy. Legal arrangements for forcing 'Environmental Impact Assessment' before establishing new geothermal power plants is required and the assessment should involve effects on both soil and water resources.

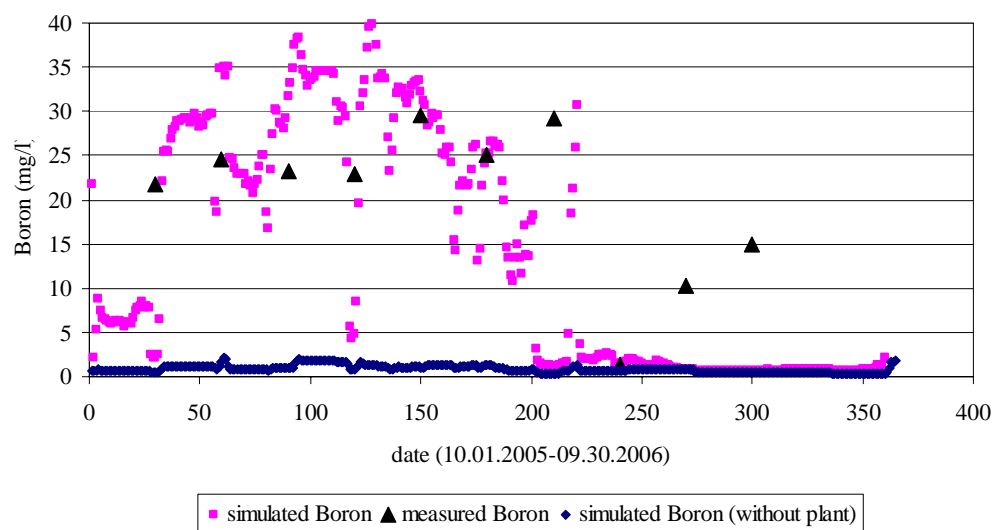


Figure 7: Comparison of the simulated and observed boron concentrations at the 12 segment of the river with and without the plant.

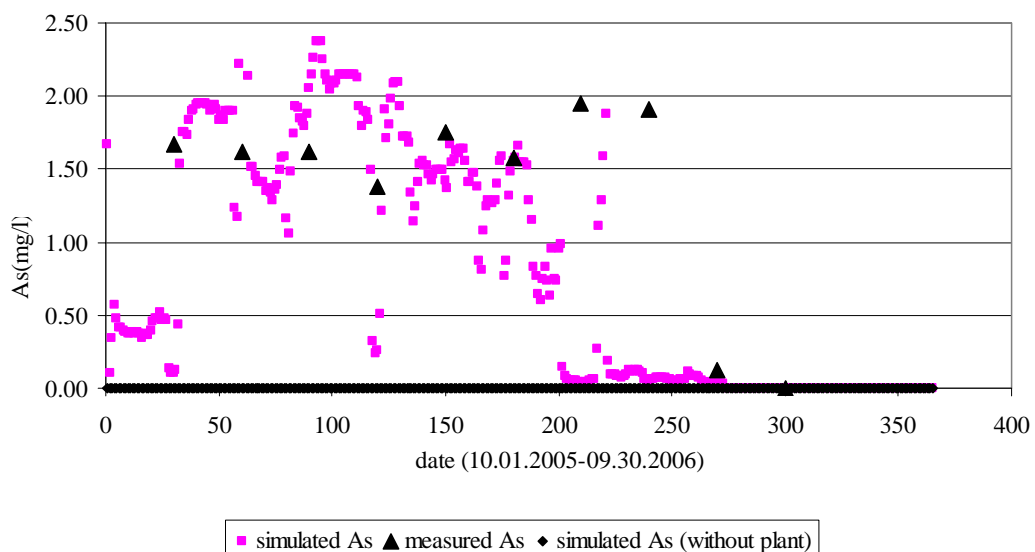


Figure 8: Comparison of the simulated and observed arsenic concentrations at the 12 segment of the river with and without the plant.

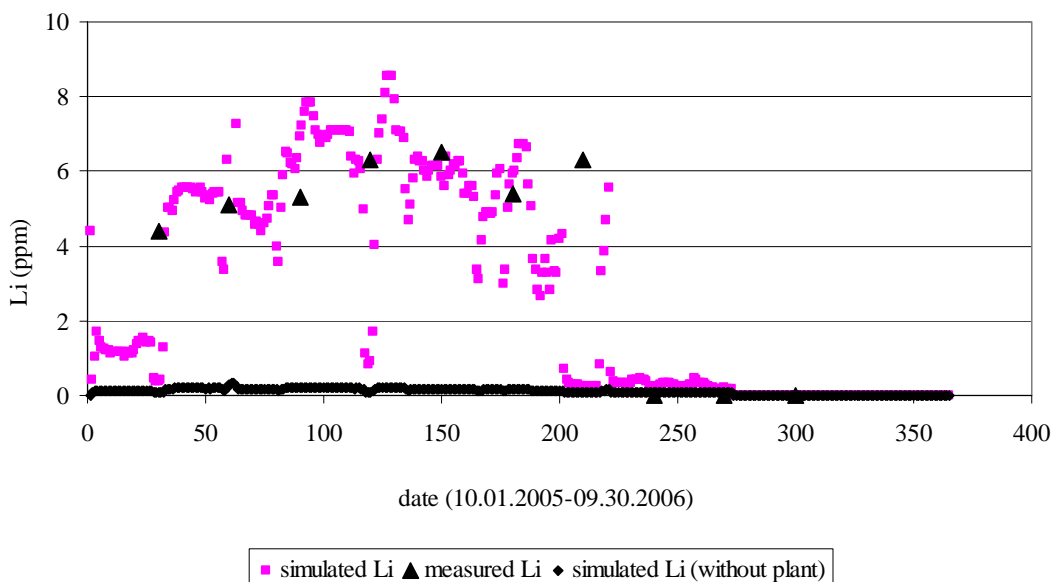


Figure 9: Comparison of the simulated and observed lithium concentrations at the 12 segment of the river with and without the plant.

ACKNOWLEDGEMENTS

Funding for this study was provided by TUBITAK (Project no: 104M301). We would like to thank to project team for their contributions. We also would like to extend our thanks to State Hydraulic Works (DSI) and Electrical Power Resources Survey and Development Administration (EIEI) for providing water quality and flow rate data.

REFERENCES

Ambrose, R.B., Wool, T., Martin, J.L.: WASP User's Manual, US Environmental Protection Agency, Environmental Research Laboratory, Athens, Georgia (1993).

Bell, V.A., George D.G., Moore R.J., and Parker, J.: Using a 1-D Mixing Model to Simulate the Vertical Flux of Heat and Oxygen in a Lake Subject to Episodic Mixing, *Ecological Modelling*, 190, (2006), 41-54.

Brown, K.L. (convener): Course on Environmental Aspects of Geothermal Development, World Geothermal Congress, Pisa-Italy, (1995), pp: 39-55, 79-95, 97-117.

Brown, K.L.: Impacts on the Physical Environment, Course on Environmental Safety and Health Issues in Geothermal Development, World Geothermal Congress, Japan, (2000), pp: 21-41, 43-56.

Gokcen, G. and Yildirim, N.: Effect of Non-condensable Gases on Geothermal Power Plant Performance. Case Study: Kizildere Geothermal Power Plant-Turkey", *International Journal of Exergy*, 5, (2008), 684-695.

Gokcen, G.: Assessment of Environmental Effects of Geothermal Development. Case Studies: Kizildere Geothermal Power Plant and Balcova Geothermal District Heating System, Project No: 104M301, TUBITAK, (2008), in Turkish.

Rybach, L.: Environmental Aspects of Geothermal Development and Utilization, and Related Legal, Institutional and Social Implications, Post-Congress Short Course on Environmental Advantages of Geothermal Energy, World Geothermal Congress, CD Transactions, Antalya, (2005), pp:297-324.

Yildirim Ozcan, N., Gokcen G.: Thermodynamic Assessment of Gas Removal Systems for Single Flash Geothermal Power Plants, *Applied Thermal Engineering*, Doi: 10.1016/j.applthermaleng.2009.04.031, (2009).

Yang, C.T.: Sediment Transport: Theory and Practice, McGraw-Hill, USA, (1996), 396 p.